

Mixture of Ionic Liquid and Organic Carbonate as an Electrolyte for LiFePO₄ Battery

Chia-Chin Chang^{1,*}, Ping-I Pan¹, Chun-Ming Wu², Hui-Ju Kao³

¹ Department of Greenergy, National University of Tainan, Tainan 70005, Taiwan

² National Synchrotron Radiation Research Center, Hsinchu, Taiwan 300

³ Department of Materials Science, National University of Tainan, Tainan 70005, Taiwan

*E-mail: ccchang@mail.nutn.edu.tw

Received: 20 January 2016 / Accepted: 12 April 2016 / Published: 4 May 2016

In the interest of expanding the available options for safe and inexpensive electrolyte in lithium ion batteries, we examined a novel electrolyte consisting of 30% IL (triethylmethylammonium bis(trifluoromethylsulfonyl)imide, N1222-TFSI) mixed with 70% commercial carbonate electrolyte (EC/DMC = 1:1 by wt%, 0.78 mol kg⁻¹ LiPF₆) to form a hybrid electrolyte. The hybrid electrolyte failed to ignite after exposure to flame, a demonstration of high thermal stability. The aluminum corrosion is inhibited in N1222-TFSI mixed carbonate electrolyte, while the N-methyl-N-propylpyrrolidinium TFSI mixed carbonate electrolyte experienced serious pitting corrosion. The electrolyte has been observed with the LiFePO₄ as positive electrode and the mesophase graphite as negative electrode in 18650 full cells. The electrochemical properties of hybrid electrolyte for the LiFePO₄ electrode at 25°C and 60°C showed improved performance at high temperature in comparison to commercial electrolyte EC/DMC (1:1 by wt%) 0.78 mol kg⁻¹ LiPF₆. Vinylene carbonate (VC) as electrolyte additive in hybrid electrolyte at 2% addition was found to enhance the cycling performance at 25°C and 60°C, however a decrease in cell performance was observed at -10°C.

Keywords: lithium-ion batteries, vinylene carbonate, ionic liquid, triethylmethylammonium bis(trifluoromethylsulfonyl) amide

1. INTRODUCTION

Lithium-ion batteries (LIBs) play an important role among power sources of choice in popular portable electronic devices: laptops, cameras, smart phones, and personal digital assistants, etc. Li-ion batteries are also highly evolved and widely used in hybrid electric vehicles (HEV), plug-in HEVs (PHEV), EVs, and energy storage systems [1]. However, safety and long cycle life are key requisites for large-size batteries in stationary applications [2].

A lithium ion cell has three major components: a graphite negative electrode, a lithium metal oxide positive electrode, and a separator soaked with liquid solution of lithium salt in carbonate solvents [3]. Orthorhombic olivine compound LiFePO_4 has been well considered as a positive electrode material for LIBs, due to its theoretical capacity of 170 mAh g^{-1} , which is environmentally benign, and does not dissociate oxygen, even at 300°C or more. LiFePO_4 possesses greater thermal stability and is suitable for large-scale rechargeable LIB applications [4, 5].

In recent years, much effort has been expended to improve the safety of LIBs. In fact, organic solvents used in commercial LIBs have poor thermal stability, low flash points and high vapor pressure [6-11]. Such poor thermal properties of the electrolyte can be controlled by using ionic liquids (ILs) to improve safety and reliability of the electrolyte for LIBs [2, 12, 13-18]. This widely studied IL is synthesized by the combination of imidazolium-based or pyrrolidinium-based cations and TFSI⁻ anion such as N-methyl-N-propylpyrrolidinium (Pyr13) salts [19-20], N-butyl-N-ethylpiperidinium salts [21], N-butyl-N-methylpyrrolidinium bis(trifluoromethylsulfonyl) -imide [2, 22] and 1-allyl-3-methylimidazolium bis(trifluoromethylsulfonyl)imide [23]. In comparison to organic solutions, IL-based electrolytes demonstrate lower ionic conductivity, with negative effects on the high charge/discharge rate and low temperature performance of batteries [2, 16, 24-25]. Adverse effects aside, the use of these mixed electrolytes allows the realization of high performance batteries to be widely studied, because of their good thermal stability, high ionic conductivity, acceptable low vapor pressure for non-flammability, and high electrochemical stability [2, 16, 22, 26-27].

LiTFSI possesses greater thermal stability, hydrolytic stability, acceptable conductivity, good electrochemical stability, and high lithium cycling performance with lithium metal [20, 27-30]. However, the practical applications of LiTFSI in the electrolytes for LIBs is limited due to the potential for corrosion at the aluminum current collector. [28, 31] It has been proposed that the mechanism of aluminum corrosion may involve the formation and diffusion of the complex ion $[\text{Al}(\text{N}(\text{SO}_2\text{CF}_3)_2)_x]^{3+x-}$ as the anion $\text{N}(\text{SO}_2\text{CF}_3)_2^-$ reacts with Al_2O_3 on the surface of the aluminum current collector during anodic current flow. [28] The solvents and salts in the examined electrolytes exhibit anti-corrosive behavior, due to having a variance in dielectric constant, dipole moment, and ionic strength. These qualities may influence the $\text{N}(\text{SO}_2\text{CF}_3)_2^-$ anion diffusion and adsorption onto the active spot of aluminum surface film, therefore preventing corrosion. [28]

In previous research, carbonate-containing compounds [32-35], sulfur-containing compounds [36-37], halogen-containing compounds [38], boron-based compounds [39, 40], and other compounds [41-45] have been proposed as electrolyte additives for LIBs. It is considered that these additives could reduce capacity fading, increase rate capability, and low- or high-temperature performance of LIBs. VC is an effective additive for the EC-based electrolyte. [35, 46-51] It has been shown that VC improves electrochemical behavior and high temperature storage, while decreasing irreversible capacity, CO_2 formation, cycling performance and the thermal stability of different Li-ion systems. [32, 35, 46-51] They proposed that the SEI layers derived from VC-containing electrolytes are formed on both the positive electrode and the negative electrode surface, forming poly alkyl Li-carbonate species that suppress both solvent and salt reaction. [52-55] However, a pronounced impact of VC on the cycling behavior of the positive electrodes remains to be found, either at room or elevated temperature. Petzl et al. [56] showed that electrolytes containing high levels of EC and VC stabilize

the SEI, and cause increased SEI-resistance as temperatures decrease (therefore favoring lithium plating).

This study examines the electrochemical properties at positive electrode when using an electrolyte consisting of triethylmethylammonium bis(trifluoromethylsulfonyl)imide (N1222-TFSI) mixed with organic solvent ethylene carbonate (EC) and dimethyl carbonate (DMC) containing a lithium salt (LiPF_6 and LiTFSI). Furthermore, corrosion of aluminum as positive electrode current collector was investigated. The interactions between either positive electrode (as LiFePO_4) or negative electrode (as mesophase graphite powder, MGP) and electrolyte mixed with ILs and organic solvents were tested for electrochemical property, rate capability, surface morphology, and cycle life at -10°C , 25°C , and 60°C . For comparison, a commercial organic electrolyte ($0.78 \text{ mol kg}^{-1} \text{ LiPF}_6$ EC/DMC, 1:1 by wt%) was also used in this study.

2.EXPERIMENTAL

2.1. Electrode preparation

The LiFePO_4 electrode was made of 84.9 wt% LiFePO_4 (Changs Ascending Ent. Co., Taiwan), 5 wt% Super P (MMM Carbon, Belgium), a 10 wt% polyvinylidene difluoride (PVdF, solef 6020, Solvy) binder dissolved in N-methyl-2-pyrrolidinone (NMP, International Specialty Products Inc.) and 0.1 wt% oxalic acid. The resulting slurry was cast on aluminum foil and dried at 100°C in a vacuum for 1 h. The negative electrodes were prepared by mixing together Super P (3 wt%), MGP (90 wt %, China Steel Chemical Corp. Taiwan), a PVdF polymer binding agent (7 wt %) and the solvent NMP, to form a slurry. The mixed slurry was coated onto copper foil ($10 \mu\text{m}$, Nippon Foil Co., Japan) and dried at 100°C . The dried electrodes were roller-compressed at room temperature to make a smooth and compact structure, and then inspected for uniform surface. Electrodes of similar thickness and weight were selected for further testing. Finally, to remove residual water content and standardize the level of hydration, the selected electrodes were stored in a glove box with oxygen and humidity content maintained below 1 ppm for more than 24 hours before electrochemical characterization.

2.2. Electrolyte preparation

Triethylmethylammonium bis(trifluoromethylsulfonyl)imide (N1222-TFSI), N-methyl-N-propyl-pyrrolidinium bis(trifluoromethylsulfonyl)imide (Pyr13-TFSI) and lithium bis(trifluoromethylsulfonyl)imide (Li-TFSI) were obtained from Kishida Chemical Co., Japan. Ethylene carbonate (EC), dimethyl carbonate (DMC) and LiPF_6 were obtained from Novolyte Technologies (BASF, Suzhou, China). The ILs-based electrolyte used $0.59 \text{ mol kg}^{-1} \text{ LiPF}_6$ and $0.19 \text{ mol kg}^{-1} \text{ LiN}(\text{SO}_2\text{CF}_3)_2$ in a ternary solvent mixture of N1222-TFSI/EC/DMC (30:28:42, w/w) (denote as NTED-electrolyte) or Pyr13-TFSI/EC/DMC (30:28:42, w/w) (denote as Pyr13ED-electrolyte). The composition of organic electrolyte was $0.78 \text{ mol kg}^{-1} \text{ LiPF}_6$ added in EC/DMC (1:1, w/w) (denote as ED-electrolyte). All electrolytes were prepared under a controlled argon atmosphere in glove boxes

with oxygen and humidity content below 1 ppm.

2.3. Coin cell and 18650-type cell

The charge–discharge curves of several coin-type cells cycled between 2.5 V and 4.2 V using a constant current of 0.13 mA/cm² (0.1C) for cell formation, and 1.3 mA/cm² (1C) for cycle test. The charge/discharge characteristics were cycle tested in a coin-type cell (CR2032) with a lithium foil counter electrode, at -10°C, 25°C and at 60°C.

A series of cylindrical 18650 lithium-ion cells composed of a positive electrode consisting of LiFePO₄ and a negative electrode consisting of MGP were tested. The positive electrode: negative electrode ratio was around 1:1.04. The reversible capacity of each cell around 1.2 Ah. The charge–discharge curve of a 18650 cell was cycled between 2.5 V and 3.8 V using a constant current of 0.24 A for cell formation, and 1.2 A for cycle test.

2.4. Electrochemical measurements

Cyclic voltammetry (CV) measurements were carried out on an Autolab electrochemical analyzer with a current sensitivity of 1 nA (Autolab PGSTAT30, Eco. Chemie). A single-compartment and triple-electrode polypropylene cell was used, and the entire apparatus was placed in the glove box. A three-electrode cell was used for cyclic voltammetry measurements, with an LiFePO₄ electrode as the working electrode and lithium foils (FMC Lithium) as counter and reference electrodes. The corrosion potential measurement of aluminum was carried out in a triple-electrode polypropylene cell after a cyclic voltammetry test. In every cycle, the potential was initially set to open circuit potential, then anodically scanned to +5.0 V and reversed to open circuit potential at 1 mV s⁻¹. [28]

Electrochemical impedance spectroscopy (EIS) was performed under open circuit voltage conditions after cycle tests of the cells. A sinusoidal amplitude modulation of ± 10 mV was carried out in a frequency range from 10 mHz to 1000 kHz, starting at high frequency and moving toward low frequency in the logarithmic scan. (Autolab PGSTAT30, Eco. Chemie)

The ionic conductivity of electrolyte was measured by impedance spectroscopy, performed with electrochemical analyzer Autolab PGSTAT30 on a two stainless steel-electrode cell. The electrolyte conductivities were measured over a wide temperature range of -20 to 20°C. The measurement of sample was equilibrated for 3 h at each temperature.

2.5. Material characterization

The surface morphology was examined by scanning electron microscope (SEM, JEOL JSM6380). The samples were cycled 200 times, then disassembled in the glove box, before the electrode was rinsed with DMC to remove salts. Finally, the electrode was dried under vacuum at room temperature for 7 hrs.

2.6. Thermogravimetric analysis (TGA)

Thermogravimetric analysis (TGA), which was used to examine changes in physical and chemical thermal properties of the mixed electrolytes, was performed by Mettler Toledo TGA/STD A851 under N_2 flux at 10 min^{-1} between 28 and 550°C . The inner diameter of the crucible and the volume of the electrolyte samples were 5 mm and ca. $30 \mu\text{L}$, respectively.

3. RESULTS AND DISCUSSION

Electrolytes containing Pyr13-TFSI and N1222-TFSI were made to evaluate the effect of electrolyte on oxidation stability of the aluminum electrode. Figure 1(I) shows the 5th CV for aluminum electrode in ED-, NTED-, and Pyr13ED-electrolytes. It was found that the oxidation stability of aluminum strongly depended on the salt. The corrosion in Pyr13ED-electrolyte was much more serious than in the other electrolytes. Microscope photograph of the aluminum foil electrode after five cycles in ED-, NTED- and Pyr13ED-electrolytes are shown in Fig. 1(II), (III), and (IV), respectively.

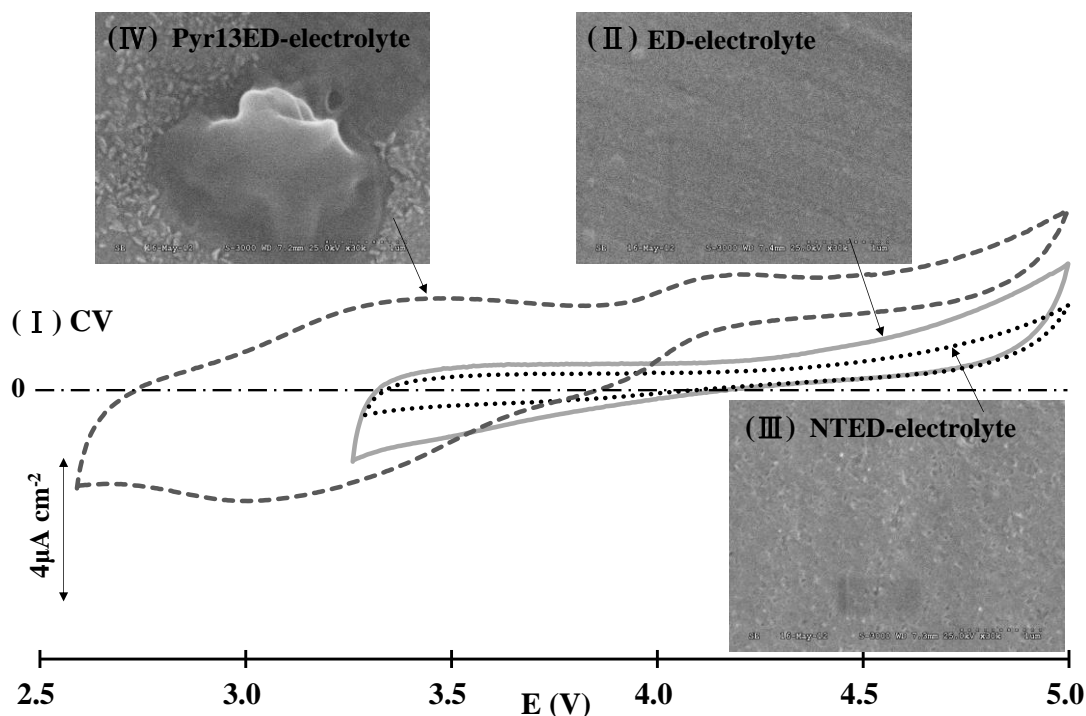


Figure 1. (I) Cyclic voltammetry of the 5th cycle for aluminum disk electrode in ED-electrolyte, NTED-electrolyte, Pyr13ED electrolyte. SEM images of aluminum after 5th cycle in (II) ED-electrolyte, (III) NTED-electrolyte, and (IV) Pyr13ED-electrolyte.

Microscope observation (Fig. 1(II)) showed no evidence of holes on the aluminum surface in the ED-electrolyte. This result shows that LiPF_6 salt forms a protective film containing AlF_3 on the aluminum surface [28], which inhibits the pitting corrosion during anodic oxidation. The mechanism

of aluminum corrosion involve the anion $\text{N}(\text{SO}_2\text{CF}_3)_2^-$ reacts with Al_2O_3 on the surface of the aluminum to form the complex ions $[\text{Al}(\text{N}(\text{SO}_2\text{CF}_3)_2)_x]^{3+x-}$. [28] In the NTED-electrolyte, Fig. 1(III) revealed that there were holes on the aluminum foil surface, but the surface was uniform and without significant erosion. This demonstrated that the aluminum foil in NTED-electrolyte incurs corrosion during the conditioning cycles, which is inhibited by AlF_3 formed from LiPF_6 during the 1st to 5th cycles. In the Pyr13ED-electrolyte, Fig. 1(IV) showed that there were holes and significant erosion precipitate on the aluminum surface, which means the aluminum electrode suffered serious corrosion by $\text{N}(\text{SO}_2\text{CF}_3)_2^-$ ion. This may be generated by the lower viscosity (i.e. liquid type at 25°C), easier dissociation, and higher structure disorder of Pyr13-TFSI than N1222-TFSI. N1222 cation is not easy associated with PF_6^- than Pyr13 cation, which may be help AlF_3 formation on aluminum foil surface. From the corrosion of aluminum foil data, we chose NTED-electrolyte for the battery performance tests.

Fig. 2 shows the result of the thermal gravimetric analysis (TGA) for various electrolytes mixed with the IL and the organic solvent. There was unobvious weight loss of the pure N1222-TFSI measured in the region of 28°C to 320°C , indicating excellent thermal stability. The weight losses in the region of 28°C to 90°C is 20%, which can be attributed to the evaporation of the DMC solvent present in the electrolyte mixture. It does not show a big difference with various amount of N1222-TFSI. Although the IL improves the thermal stability of the EC/DMC electrolyte, the initial weight loss from 90 to 170°C is attributed to the decomposition of LiPF_6 and organic solvents in the mixtures. These results are similar to those obtained previously by Zaghbi et al. [10] The remaining weight loss was $<10\%$ at around 200°C , revealed to the EC/DMC system due to the high volatility. Improved thermostability of the IL-based electrolytes appeared above 150°C , and the electrolyte weight decreased to 60% and 40% at the plateau region of $200\text{--}380^\circ\text{C}$ for 50 wt% and 30 wt% IL-based electrolytes, respectively.

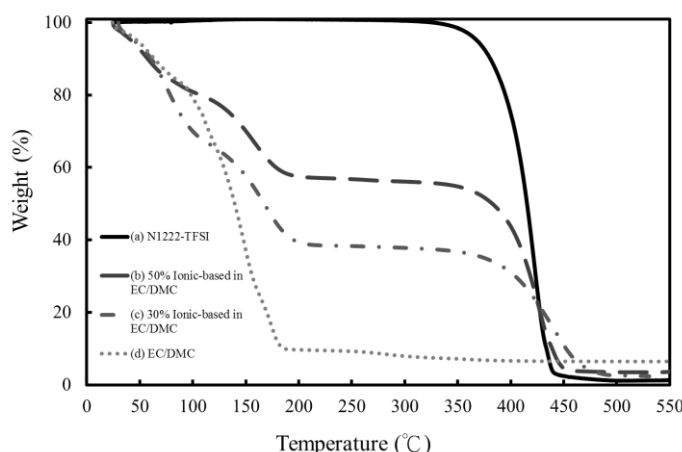


Figure 2. Thermogravimetric analysis: (a) N1222-TFSI ; (b) 50 wt% ionic liquid in EC/DMC 1/1 by weight $0.59 \text{ mol kg}^{-1} \text{ LiPF}_6$ and $0.19 \text{ mol kg}^{-1} \text{ LiN}(\text{SO}_2\text{CF}_3)_2$; (c) 30% ionic liquid in EC/DMC 1/1 by weight $0.59 \text{ mol kg}^{-1} \text{ LiPF}_6$ and $0.19 \text{ mol kg}^{-1} \text{ LiN}(\text{SO}_2\text{CF}_3)_2$; (d) EC/DMC 1/1 by weight $0.78 \text{ mol kg}^{-1} \text{ LiPF}_6$. Temperature range: room temperature to 550°C , Scan rate: $10^\circ\text{C min}^{-1}$.

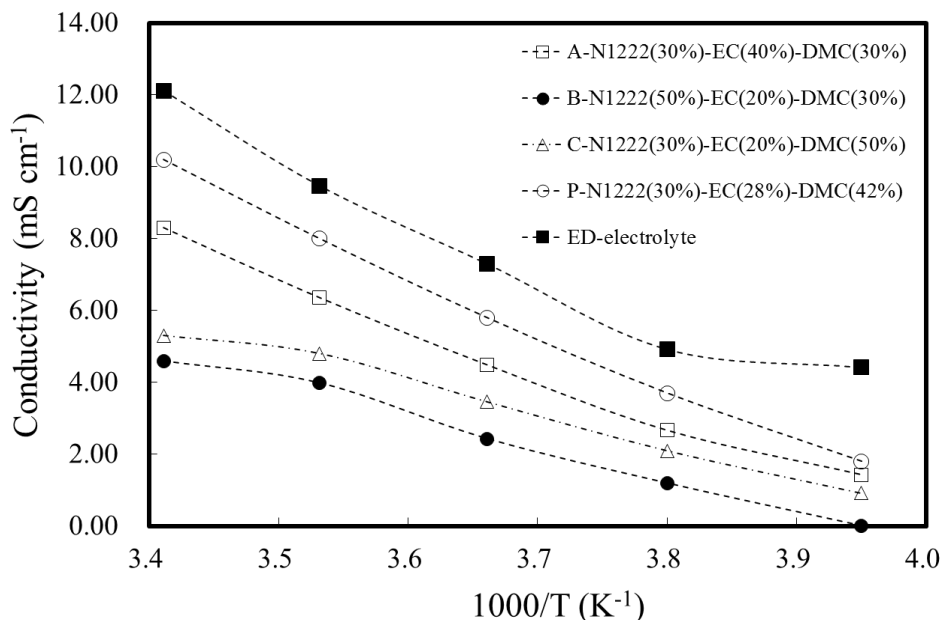


Figure 3. Conductivity data at 20 to -20°C of ED-electrolyte and solutions with different wt% of N1222-TFSI, EC, and DMC

The conductivities of various N1222-TFSI, EC, and DMC mixtures with LiTFSI and LiPF_6 at 20 to -20°C , measured via ac impedance spectroscopy, are shown in Fig. 3. These conductivity values are significantly lower than that of conventional carbonate electrolytes (as ED-electrolyte) (10^{-3} S/cm) when ILs or DMC content is high, but the mixture of N1222-TFSI/EC/DMC (30:28:42, w/w) electrolyte are comparable to that of IL-based electrolytes [57]. The ionic conductivity of mixture of N1222-TFSI/EC/DMC (30:28:42, w/w) electrolyte at 20°C is 10 mS cm^{-1} which is higher than that of 1-ethyl-3-methylimidazolium-bis(fluorsulfonyl)imide-TFSI/EC/DEC (30:35:35, w/w) (8.6 mS cm^{-1}) [10]. The mixture of N1222-TFSI/EC/DMC (30:28:42, w/w) electrolyte exhibits enough conductivity for use in LIBs. Some interesting properties were observed in our studies on these mixture electrolytes, as reported below.

The cyclic voltammograms of the LiFePO_4 electrode in ED-electrolyte, NTED-electrolyte, and NTED-electrolyte with 1% VC are illustrated in Fig. 4(I). Fig. 4(I) shows two sharp peaks corresponding to the $\text{Fe}^{3+}/\text{Fe}^{2+}$ redox couple observed during the first cycle at a scan rate 0.1 mV s^{-1} . Peak voltage difference ($E_{\text{pc}}-E_{\text{pa}}$) between the anodic and cathodic peak was found to be 0.224 V, 0.391 V, and 0.415 V for the ED-electrolyte, NTED-electrolyte, and NTED-electrolyte with 1% VC, respectively. The peak current of ED-electrolyte is higher than that of NTED-electrolyte with/without VC. The high peak voltage difference and low current peaks can be attributed to the low ionic conductivity of NTED-electrolyte.

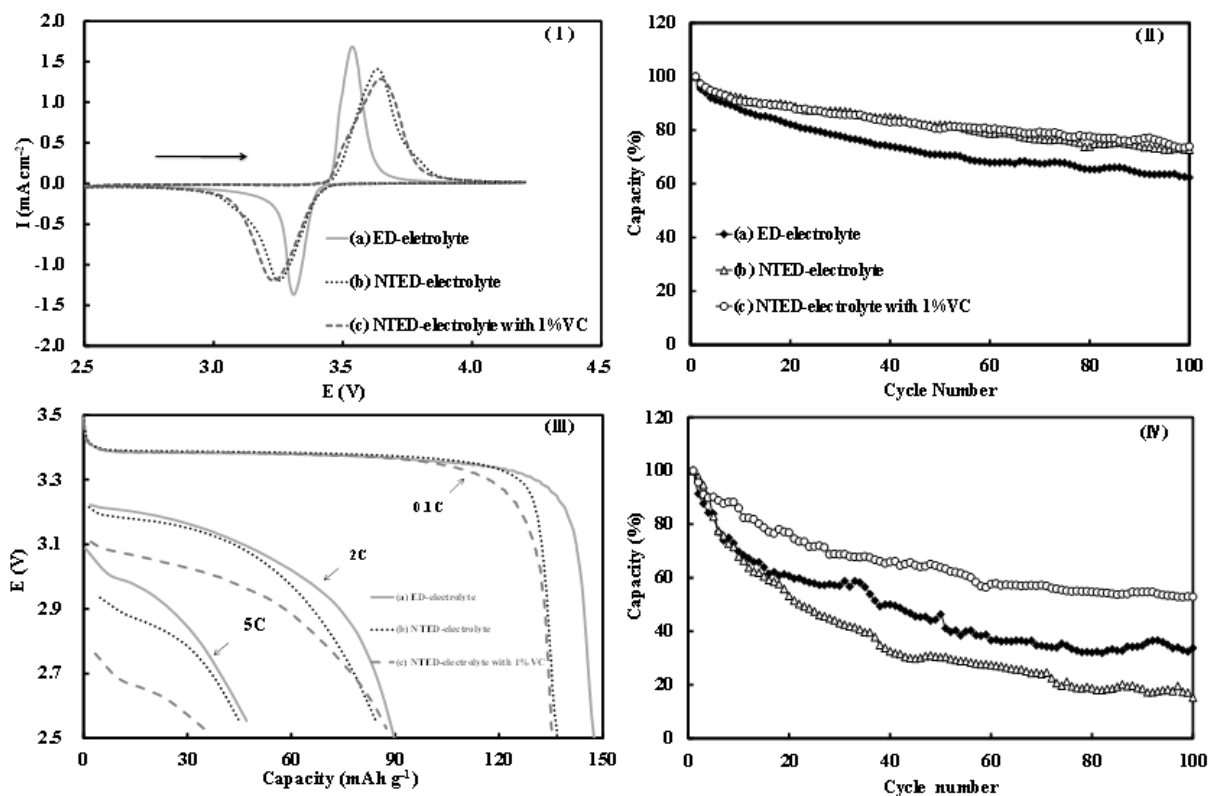


Figure 4. LiFePO₄ electrode in: (a) ED-electrolyte, (b) NTED-electrolyte, and (c) NTED-electrolyte with 1% VC : (I) Cyclic voltammetry between 2.5 to 4.2 V at a scan rate of 0.1 mVs⁻¹; (II) Cycle performances at 25°C and 1C rate; (III) Discharge curves of rate capability at various current rates from 0.1 to 5.0 C; (IV) Cycle performances at 60°C and 1C rate.

The capacity fading of the LiFePO₄ electrode in NTED-electrolytes with 1% VC at 1.0 C rate capability is shown in Fig. 4(II). The capacity fading of LiFePO₄ after 100 cycles in NTED-electrolyte was insignificantly different from that of ED-electrolyte. The discharge rate capabilities tested were obtained at various rates from 0.13 mA/cm² (C/10) to 6.5 mA/cm² (5C), with a constant C/10 charging rate (Fig. 4(III)). The results showed that the rate capability of LiFePO₄ in NTED-electrolyte was lower than that of ED-electrolyte. However, the rate capability of LiFePO₄ in the NTED-electrolyte is better than that in butylmethylpyrrolidinium-TFSI with 10% gamma-butyrolactone electrolyte [58]. An examination of Fig. 4(III) shows that the working voltage of NTED-electrolyte was lower than that of ED-electrolyte. This result showed that the ionic conductivity of NTED-electrolyte was lower than that of ED-electrolyte at 25°C. However, the working voltage of NTED-electrolyte with 1% VC was lower than that of NTED-electrolyte without 1% VC at 25°C, which may be induced by increased formation of solid electrolyte interface (SEI) films by VC on both the positive and the negative electrode surfaces. The cycling performance of LiFePO₄/Li cells with various electrolytes at 60°C is shown in Fig. 4(IV). These results show that VC additive in NTED-electrolyte can significantly enhance the cycling performance of the LiFePO₄ electrode at high temperature, due to the complete SEI films formed on the electrode surface.

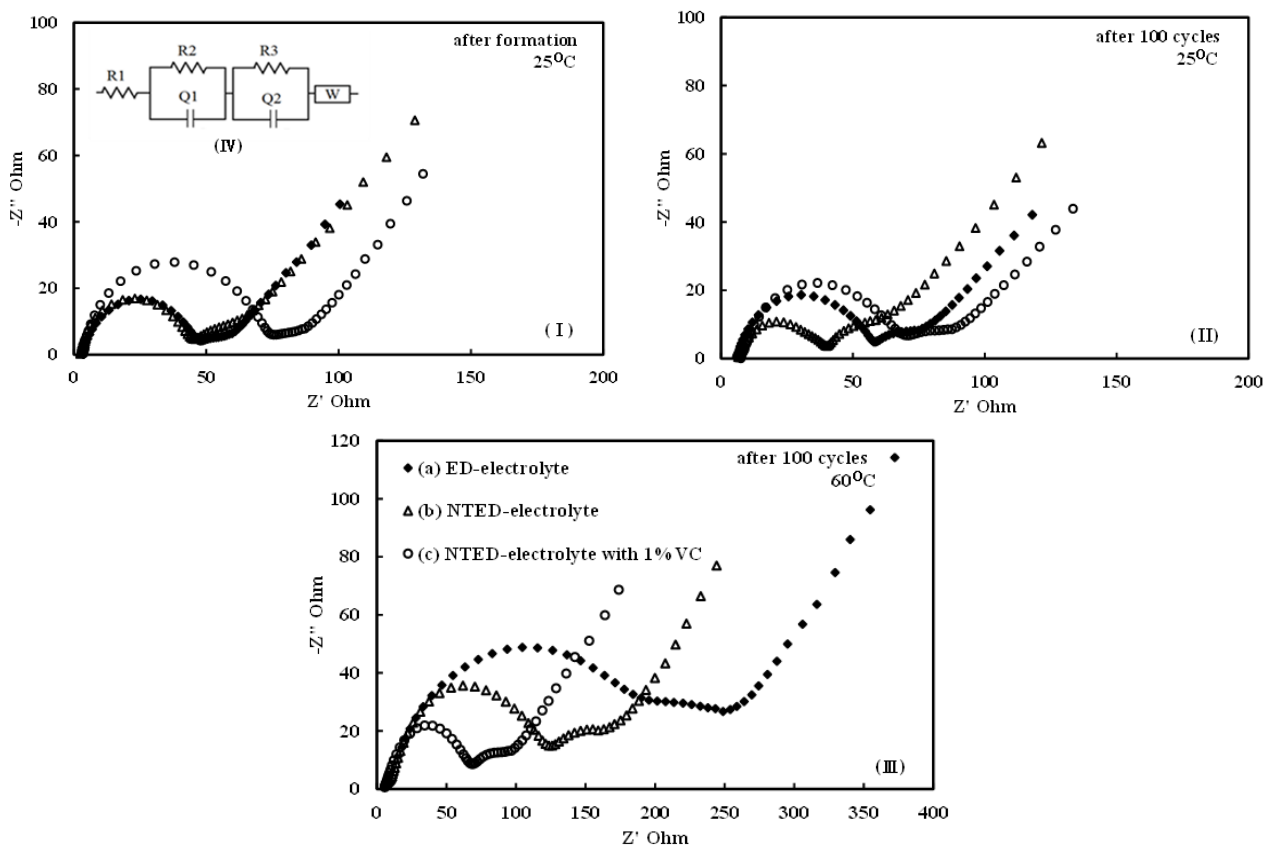


Figure 5. Impedance spectra of LiFePO₄/Li cells in different electrolytes, (I) after formation at 25°C, (II) after 100 cycles at 25°C, and (III) after 100 cycles at 60°C. (IV) Equivalent circuit module of impedance parameters.

The electrochemical impedance spectroscopy (EIS) results for LiFePO₄/Li cells after formation, 100 cycles at 25°C, and 100 cycles at 60°C, are shown in the Nyquist plot Fig. 5(I), 5(II), and 5(III), respectively. The high-frequency resistance semicircle represents the external circuit (R1), medium frequency resistance region represents the SEI film (R2), and low-frequency resistance semicircle represents the charge-transfer resistance (R3). Data is simulated by using the model in Fig. 5(IV) and shown in Table 1.

Table 1. Impedance parameters of LiFePO₄/Li cells in different electrolytes after formation at 25°C, after 100 cycles at 25°C, and after 100 cycles at 60°C.

	ED-electrolyte (ohm)			NTED-electrolyte (ohm)			NTED-electrolyte with 1% VC (ohm)		
	R1	R2	R3	R1	R2	R3	R1	R2	R3
25°C after formation	4.7	52.4	22.8	4.8	50.4	24.1	5.2	84.8	26.7
25°C after 100 cycles	7.8	67.4	30.0	8.3	48.9	34.4	9.1	79.5	31.8
60°C after 100 cycles	11.3	213.4	145.6	9.5	167.8	45.9	7.5	87.4	32.6

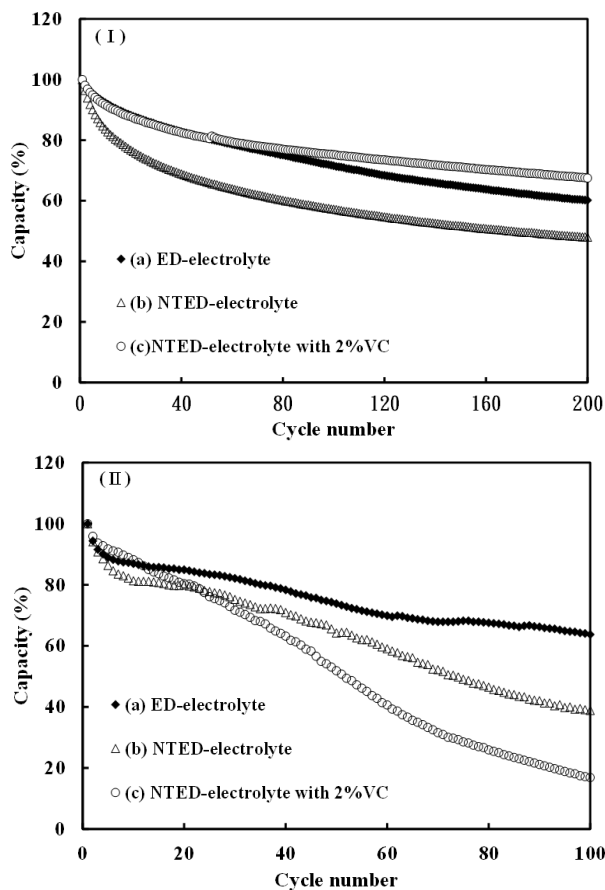


Figure 6. Capacity fading ratio of LiFePO₄/MGP 18650 full cell at (I) 60°C and (II) -10°C in: (a) ED-electrolyte, (b) NTED-electrolyte, and (c) NTED-electrolyte with 2% VC.

The R1 data represent the series resistance of current collector, materials and electrolyte. The R2 data results demonstrated that the resistances of SEI films of LiFePO₄/Li cell in NTED-electrolyte with 1% VC after formation and 100 cycles at 25°C were higher than that in the other electrolytes. However, the lithium anode and LiFePO₄ surface had grown thicker SEI film at 60°C after 100 cycles in both the ED-electrolyte and NTED-electrolyte without VC. The VC additive in the NTED-electrolyte showed the similar impedance values in the low-frequency region (R3) after 100 cycles between 25°C and 60°C. The R3 impedance of LiFePO₄ at 60°C in the NTED-electrolyte with 1% VC were lower than that in the ED-electrolyte, which can be explained by observing the VC additive enhancing the formation of a complete SEI film on the electrode surface and showing improved ion transformation for lithium cations. The impedance data demonstrates that the VC additive not only improves SEI film formation, but also protects anode, which will extend the life cycle at high operating temperature.

According to the above LiFePO₄/Li cell test results, the N1222-TFSI mixed EC/DMC 0.59 mol kg⁻¹ LiPF₆ and 0.19 mol kg⁻¹ LiN(SO₂CF₃)₂ electrolyte have good electrochemical performance. In order to understand the behavior of the NTED-electrolyte in the 18650 full cell condition, the MGP negative and LiFePO₄ positive electrodes were used in the cell design. To aid the negative electrode and the positive electrode materials in the formation of SEI films, VC content was increased to 2%.

Fig. 6(I) shows the resultant cycling performance of 18650 LiFePO₄/MGP cells with ED-electrolyte, NTED-electrolyte, and NTED-electrolyte with 2% VC electrolyte at 60°C. A comparison of results shows that the cycling performance of 18650 LiFePO₄/MGP cells with NTED-electrolyte containing 2% VC electrolyte are better than that with ED-electrolyte cells after 200 cycles at 60°C. The NTED-electrolyte with VC additive may assist in SEI formation on the LiFePO₄ and MGP surface, and improve the cycling performance at 60°C.

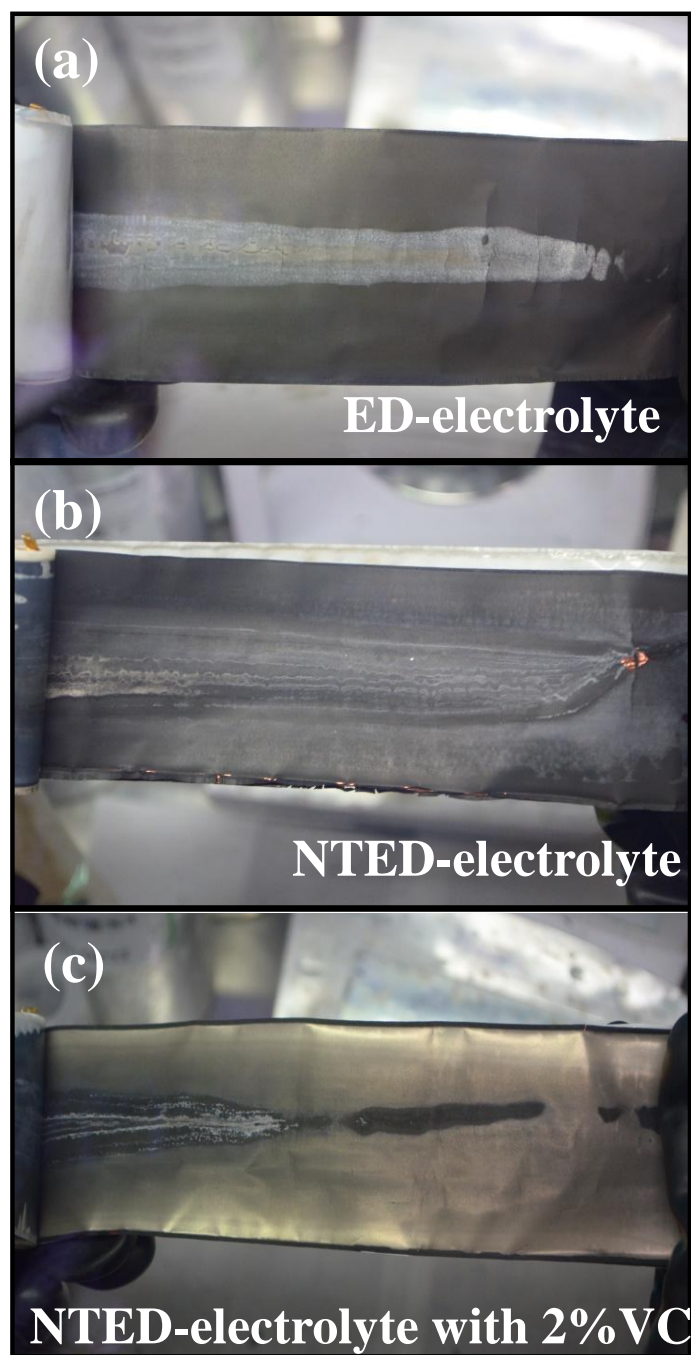


Figure 7. A photograph of the MGP electrode after 100 cycles with different electrolytes: (A) ED-electrolyte, (B) NTED-electrolyte, (C) NTED-electrolyte with 2% VC.

The cycling performance of 18650-type $\text{LiFePO}_4/\text{MGP}$ cells with ED-electrolyte, NTED-electrolyte, NTED-electrolyte with 2% VC at -10°C are shown in Fig. 6(II). Compared to other electrolytes at -10°C , NTED-electrolyte with 2% VC cell shows a significant capacity decrease after 100 cycles. This result shows that the VC additive may create complete SEI films, which have high resistance under -10°C , due to the lithium plating on the negative electrode surface as shown in Figure 7. Likewise, Petzl et al. [59-60] showed that high EC- and VC- volume in the electrolyte stabilize the SEI, but also cause increased SEI resistance at lower temperature (in support of lithium plating).

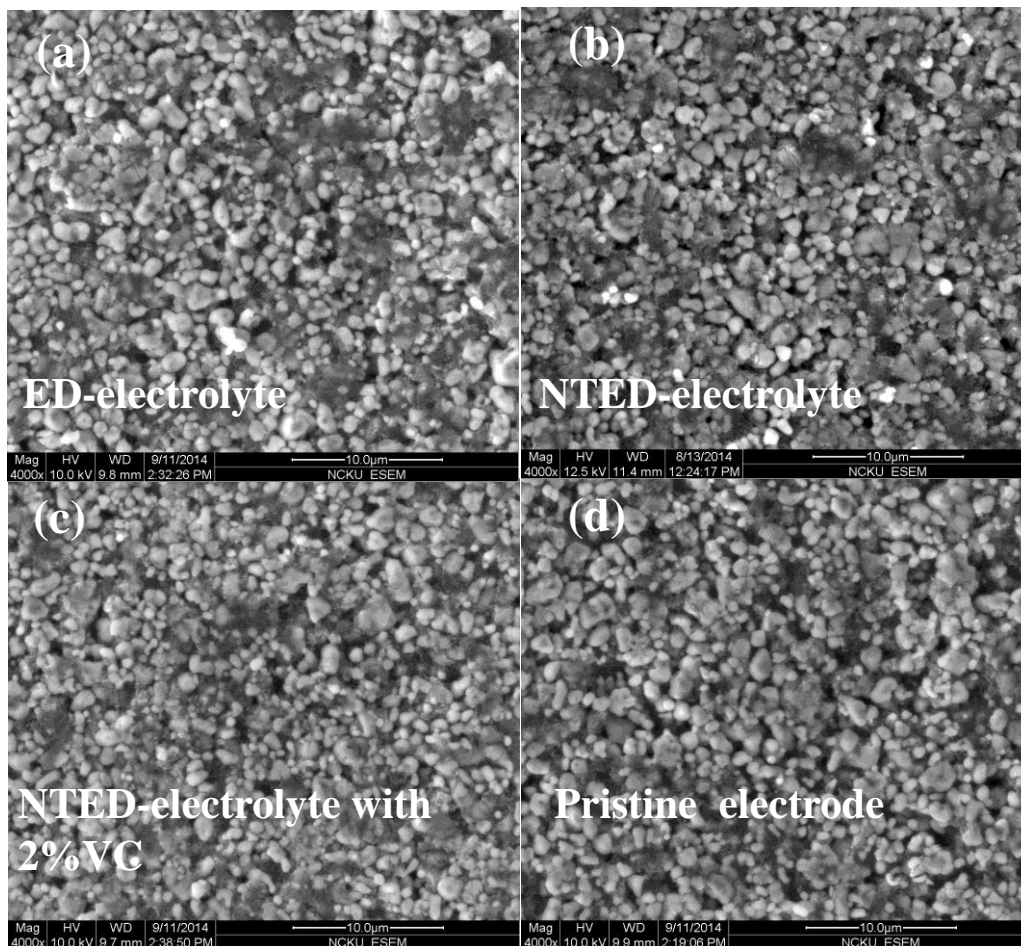


Figure 8. SEM images of the LiFePO_4 electrode after 200 cycles at 60°C in: (A) ED-electrolyte, (B) NTED-electrolyte, (C) NTED-electrolyte with 2% VC, and (D) pristine LiFePO_4 electrode.

Fig. 8 shows the scanning electron microscope (SEM) images of the LiFePO_4 electrode in various electrolytes after 200 cycles at 60°C . There were non-significant differences between NTED-electrolyte (Fig. 8 (A), (B), and (C)) and the pristine LiFePO_4 electrode (Fig. 8 (D)). These results showed that NTED-electrolyte had a non-significant reaction between the electrolyte and LiFePO_4 electrode surface at 60°C . SEM image of the MGP in various electrolytes after 200 cycles at 60°C are shown in Fig. 9. Comparing the SEM results (Fig. 9 (A)-(D)), the surface morphology of MGP electrode in NTED-electrolyte with 2% VC incurred more particle roughness than that in ED-electrolyte. They demonstrate that the VC additive significantly reduces the decomposition reaction

between electrolyte and MGP electrode surface after 200 cycles at 60°C. This consequence can explain why the VC additive affects the SEI formation and enhances the cycling performance of 18650 full cells at a high temperature of 60°C.

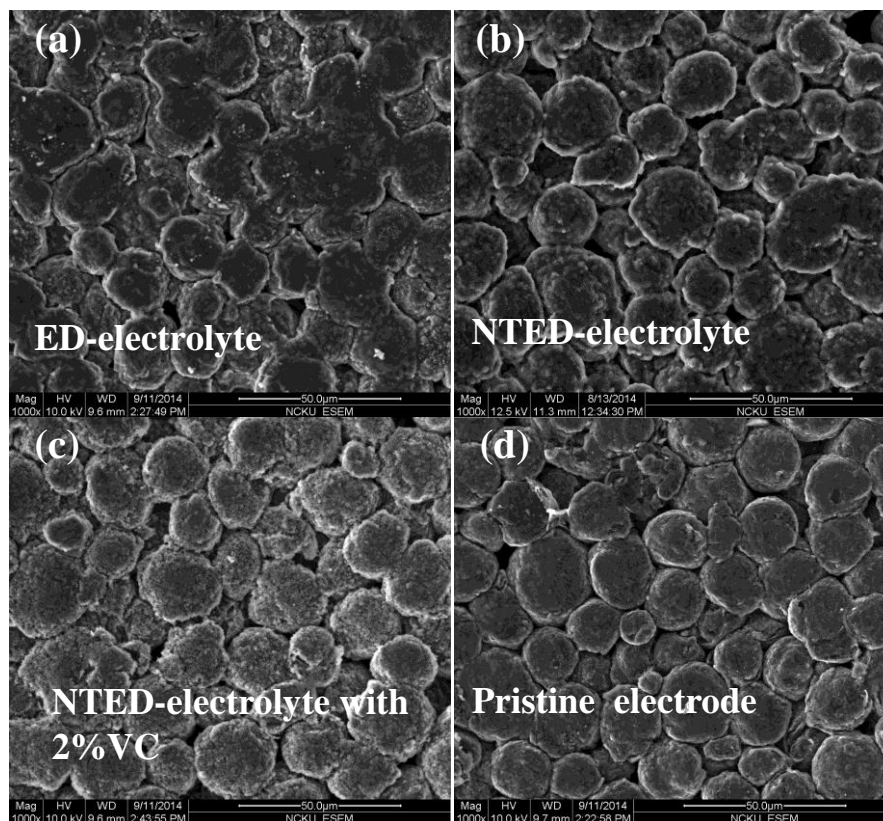


Figure 9. SEM images of the MGP electrode after 200 cycles at 60°C in: (A) ED-electrolyte, (B) NTED-electrolyte, (C) NTED-electrolyte with 2% VC, and (D) pristine MGP electrode.

4. CONCLUSIONS

The tested electrolytes proved to be safe and efficient, while demonstrating corrosion resistance, improved cyclability at high temperature, and adequate conductivity. IL (triethylmethylammonium bis(trifluoromethylsulfonyl) amide, N1222-TFSI) (30%) is mixed with commercial carbonate electrolyte (EC/DMC = 1:1 by wt%) (70%) and 0.78 mol kg⁻¹ LiPF₆ salt (denote NTED-electrolyte) to form a hybrid electrolyte with/without vinylene carbonate (VC) additive. The corrosion of aluminum foil was insignificant, while that in Pyr13-ED electrolyte was obvious. The hybrid electrolyte showed improved cyclability in the presence of VC at 25°C and 60°C for LiFePO₄/Li half-cell. From the 18650 full cell test results, the cell performance of hybrid electrolyte for LiFePO₄ electrode at 60°C is equivalent to commercial electrolyte EC/DMC 0.78 mol kg⁻¹ LiPF₆ salt; but, it has diminished cell performance at -10°C. When vinylene carbonate (VC) 2% as electrolyte additive in hybrid electrolyte was added, VC showed the capacity to enhance the cycling

performance at 25°C and 60°C. However, it has poor performance at -10°C, which was caused by the SEI layer formed on the graphite surface in IL with VC.

ACKNOWLEDGEMENTS

Financial support was provided by the HOPAX Chemicals Mfg. Co., Aleees Eco Ark Co. Ltd., and the Ministry of Science and Technology of Taiwan under the following contracts: MOST 104-2811-E024-001, MOST 104-2622-E024-001 and MOST 105-3113-E-006-019 –CC2.

References

1. T. Tanaka, K. Ohta, N. Arai, *J. Power Sources*, 97 (2001) 2.
2. C. Arbizzani, G. Gabrielli, M. Mastragostino, *J. Power Sources*, 196 (2011) 4801.
3. L. Lombardo, S. Brutti, M.A. Navarra, S. Panero, P. Reale, *J. Power Sources*, 227 (2013) 8.
4. H.C. Wu, C.Y. Su, D.T. Shieh, M.H. Yang, N.L. Wu, *Electrochem. Solid-State Lett.*, 9 (2006) A537.
5. H. Srour, H. Rouault, C. Santini, *J. Electrochem. Soc.*, 160 (2013) A66.
6. D.H. Doughty, E.P. Roth, C.C. Crafts, G. Nagasubramanian, G. Henriksen, K. Amine, *J. Power Sources*, 146 (2005) 116.
7. H. Nakagawa, Y. Fujino, S. Kozono, Y. Katayama, T. Nukuda, H. Sakaebe, H. Matsumoto, K. Tatsumi, *J. Power Sources*, 174 (2007) 1021.
8. C. Yan, L. Zaijun, Z. Hailang, F. Yinjun, F. Xu, L. Junkang, *Electrochim. Acta*, 55 (2010) 4728.
9. B.S. Lalia, N. Yoshimoto, M. Egashira, M. Morita, *J. Power Sources*, 195 (2010) 7426.
10. A. Guerfi, M. Dontigny, P. Charest, M. Petitclerc, M. Lagacé, A. Vijn, K. Zaghbi, *J. Power Sources*, 195 (2010) 845.
11. D.D. MacNeil, Z. Lu, Z. Chen, J.R. Dahn, *J. Power Sources*, 108 (2002) 8.
12. N. Salem, Y. Abu-Lebdeh, *J. Electrochem. Soc.*, 161 (2014) A1593.
13. L.A. Blanchard, D.Hancu, E.J. Beckman, J.F. Brennecke, *Nature*, 399 (1999) 28.
14. H. Matsumoto, H. Sakaebe, K. Tatsumi, M. Kikuta, E. Ishiko, M. Kono, *J. Power Sources*, 160 (2006) 1308.
15. B. Garcia, S. Lavalle, G. Perron, C. Michot, M. Armand, *Electrochim. Acta*, 49 (2004) 4583.
16. M. Montanino, M. Moreno, M. Carewcka, G. Maresca, E. Simonetti, R. Lo Presti, F. Alessandrini, G. B. Appetecchi, *J. Power Sources*, 269 (2014) 608.
17. C.Y. Lin, C.C. Chang, *J. Chin. Chem. Soc.*, 59 (2012) 1244.
18. Y. Ishihara, K. Miyazaki, T. Fukutsuka, T. Abe, *J. Electrochem. Soc.*, 161 (2014) A1939.
19. A. Farnicola, F. Croce, B. Scrosati, T. Watanabe, H. Ohno, *J. Power Sources*, 174 (2007) 342.
20. A. I. Bhatt, A. S. Best, J. Huang, A. F. Hollenkamp, *J. Electrochem. Soc.*, 157 (2010) A66.
21. A. Farnicola, F.C. Weise, S.G. Greenbaum, J. Kagimoto, B. Scrosati, A. Soletto, *J. Electrochem. Soc.*, 156 (2009) A514.
22. R. S. Kühnel, N. Böckenfeld, S. Passerini, M. Winter, A. Balducci, *Electrochim. Acta*, 56 (2011) 4092.
23. M. Wang, Z. Shan, J. Tian, K. Yang, X. Liu, H. Liu, K. Zhu, *Electrochim. Acta*, 95 (2013) 301.
24. K. Tsunashima, M. Sugiya, *Electrochem. Commun.*, 9 (2007) 2353.
25. Y. An, P. Zuo, X. Cheng, L. Liao, G. Yin, *Int. J. Electrochem. Soc.*, 6 (2011) 2398.
26. J. K. Kim, A. Matic, J. H. Ahn, P. Jacobsson, *RSC Adv.*, 2 (2012) 9795.
27. A. S. Best, A. I. Bhatt, A. F. Hollenkamp, *J. Electrochem. Soc.*, 157 (2010) A903.
28. X. Wang, E. Yasukawa, S. Mori, *Electrochim. Acta*, 45 (2000) 2677.
29. C. W. Schmidt, S. A. Symes, in *The analysis of burned human remains*, p. 2, Academic Press, ISBN 0-12-37250-0 (2008).
30. T. Placke, O. Fromm, S. F. Lux, P. Bieker, S. Rothermel, H.-W. Meyer, S. Passerini, M. Winter, *J.*

- Electrochem. Soc.*, 159 (2012) A1755.
31. M. Morita, T. Shibata, N. Yoshimoto, M. Ishikawa, *J. Power Sources*, 119 (2003) 784.
 32. H. Yoshitake, K. Abe, T. Kitakura, J.B. Gong, Y.S. Lee, H. Nakamura, M. Yoshio, *Chem. Lett.*, 32 (2003) 134.
 33. K.C. Möller, H.J. Santner, W. Kern, S. Yamaguchi, J.O. Besenhard, M. Winter, *J. Power Sources*, 119 (2003) 561.
 34. H.J. Santner, K.C. Möller, J. Ivanò, M.G. Ramsey, F.P. Netzer, S. Yamaguchi, J.O. Besenhard, M. Winter, *J. Power Sources*, 119 (2003) 368.
 35. M. Holzapfel, A. Wursig, W. Scheifele, J. Vetter, and P. Novak, *J. Power Sources*, 174 (2007) 1156.
 36. Y. Ein-Eli, *J. Electroanal. Chem.*, 531 (2002) 95.
 37. K. C. Höglström, S. Malmgren, M. Hahlin, H. Rensmo, F. Thébault, P. Johansson, K. Edström, *J. Phys. Chem.*, C 117 (2013) 23476.
 38. A. Naji, J. Ghanbaja, P. Willmann, D. Billaud, *Electrochim. Acta*, 45 (2000) 1893.
 39. C.C. Chang, T.K. Chen, L.J. Her and G.T.K. Fey, *J. Electrochem. Soc.*, 156 (2009) A828.
 40. C.C. Chang and T.K. Chen, *J. Power Sources*, 193 (2009) 834.
 41. S. Komaba, B. Kaplan, T. Ohtsuka, Y. Kataoka, N. Kumagai, H. Groult, *J. Power Sources*, 119 (2003) 378.
 42. K.C. Möller, T. Hodal, W.K. Appel, M. Winter, J.O. Besenhard, *J. Power Sources*, 97 (2001) 595.
 43. Y. Matsuo, K. Fumita, T. Fukutsuka, Y. Sugie, H. Koyama, K. Inoue, *J. Power Sources*, 119 (2003) 373.
 44. H. Ota, A. Kominato, W.J. Chun, E. Yasukawa, S. Kasuya, *J. Power Sources*, 119 (2003) 393.
 45. S. Yoon, H. Kim, J. J. Cho, Y. K. Han, H. Lee, *J. Power Sources*, 244 (2013) 711.
 46. M. Contestabile, M. Morselli, R. Paraventi, and R. J. Neat, *J. Power Sources*, 119 (2003) 943.
 47. M. Holzapfel, C. Jost, A. Prodi-Schwab, F. Krumeich, A. Wursig, H. Buqa, and P. Novak, *Carbon*, 43 (2005) 1488.
 48. T. Sasaki, T. Abe, Y. Iriyama, M. Inaba, and Z. Ogumi, *J. Electrochem. Soc.*, 152 (2005) A2046.
 49. H.-C. Wu, C.-Y. Su, D.-T. Shieh, M.-H. Yang, and N.-L. Wu, *Electrochem. Solid-State Lett.*, 9 (2006) A537.
 50. E.G. Shim, T.H. Nam, J.G. Kim, H.S. Kim, and S.I. Moon, *J. Power Sources*, 172 (2007) 901.
 51. J. Y. Eom, I. H. Jung, J. H. Lee, *J. Power Sources*, 196 (2011) 9810.
 52. H. Ota, K. Shima, M. Ue, and J.-I. Yamaki, *Electrochim. Acta*, 49 (2004) 565.
 53. H. Ota, Y. Sakata, A. Inoue, and S. Yamaguchi, *J. Electrochem. Soc.*, 151 (2004) A1659.
 54. D. Aurbach, K. Gamolsky, B. Markovsky, Y. Gofer, M. Schmidt, and U. Heider, *Electrochim. Acta*, 47 (2002) 1423.
 55. D. Aurbach, B. Markovsky, A. Rodkin, E. Levi, Y. S. Cohen, H.-J. Kim, and M. Schmidt, *Electrochim. Acta*, 47 (2002) 4291.
 56. M. Petzl, M.A. Danzer, *J. Power Sources*, 254 (2014) 80.
 57. S. Fang, Z. Zhang, Y. Jin, L. Yang, S. Hirano, K. Tachibana, S. Katayama, *J. Power Sources*, 196 (2011) 5637.
 58. N. Wongittharom, C.-H. Wang, Y.-C. Wang, G. T.-K. Fey, H.-Y. Li, T.-Y. Wu, T.-C. Lee, J.-K. Chang, *J. Power Sources* 260 (2014) 268.
 59. M.C. Smart, B.V. Ratnakumar, L. Whitcanacka, K. Chin, M. Rodriguez, S. Surampudi, *Aerosp. Electron. Syst. Mag. IEEE*, 17 (2002) 16.
 60. M.C. Smart, B.V. Ratnakumar, *J. Electrochem. Soc.*, 158 (2011) A379.